analytical chemistry

Article

pubs.acs.org/ac

Picking up the Pieces: A Generic Porous Si Biosensor for Probing the Proteolytic Products of Enzymes

Giorgi Shtenberg,[†] Naama Massad-Ivanir,[‡] Oren Moscovitz,[∥] Sinem Engin,[⊥] Michal Sharon,[∥] Ljiljana Fruk,*[,⊥] and Ester Segal*[,‡,§]

[†]The Inter-Departmental Program of Biotechnology, [‡]Department of Biotechnology and Food Engineering, [§]The Russell Berrie Nanotechnology Institute, Technion—Israel Institute of Technology, Haifa 32000, Israel

[∥]Department of Biological Chemistry, Weizmann Institute of Science, Rehovot 76100, Israel

[⊥]DFG—Center for Functional Nanostructures, Karlsruhe Institute of Technology, Karlsruhe 76131, Germany

Supporting Information

ABSTRACT: A multifunctional porous Si biosensor that can both monitor the enzymatic activity of minute samples and allow subsequent retrieval of the entrapped proteolytic products for mass spectrometry analysis is described. The biosensor is constructed by DNA-directed/reversible immobilization of enzymes onto a Fabry–Pérot thin film. We demonstrate high enzymatic activity levels of the immobilized enzymes (more than 80%), while maintaining their specificity. Mild dehybridization conditions allow enzyme recycling and facile surface regeneration for consecutive biosensing analysis. The catalytic activity of the immobilized enzymes is monitored in real time by reflective interferometric Fourier transform spectroscopy. The real-time analysis of minute quantities of enzymes (concentrations at least 1 order of magnitude lower, 0.1 mg mL^{-1}, in comparison to previous reports, 1 mg mL^{-1}), in particular proteases, paves the way for substrate profiling and the identification of cleavage sites. The biosensor configuration is compatible with common proteomic methods and allows for a successful downstream mass spectrometry analysis of the reaction products.

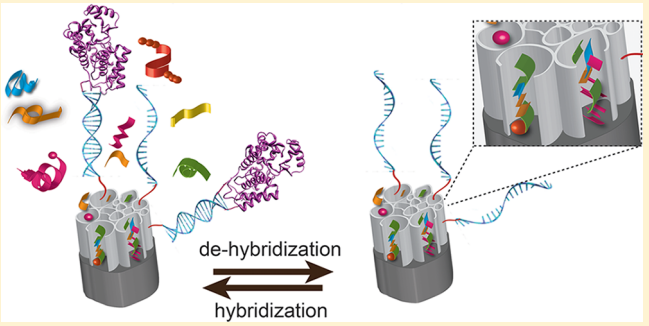

Nanostructured porous Si (PSi) has emerged as a promising material for optical biosensing applications due to its large internal surface area and tunable optical properties.[1] PSi-based interferometers, in which a change in refractive index of the solution contained within the porous nanostructure can be measured, allow for label-free detection of a variety of biomolecular interactions.[2] Despite the vast innovation in PSi biosensor technology there are only a few reports of PSi-based platforms that address substrate specificity of enzymatic reactions.[3,4] Orosco et al.[5] designed an optical biosensor for quantifying protease activity of pepsin by forming a layer of zein protein on top of a PSi photonic crystal. Distinct color changes are observed due to the infiltration of the protein's digestion products into the pores. In a more recent study, a double-layer PSi interferometer was used for isolation and real-time quantification of protease digestion products, when proteases are trapped within the nanostructured pores.[6] The later sensing format involved nonspecific immobilization of the protease in the pores,[6] while other designs used covalent attachment of the substrate to the PSi transducer.[7−9] These exciting proof-of-concept studies demonstrated the applicability of PSi optical nanostructures to monitor enzymes activity. Nevertheless, several challenges remain to render existing biosensors into more powerful and versatile platforms. First, the design of previous biosensors involves the immobilization of the substrate to or onto the PSi transducer, while the studied protease is incubated with the activated surface and cannot be retrieved for reuse, which is important when both the enzyme and the substrate to be analyzed are available in minute amounts.[10,11] Second, most current biosensing schemes require prior knowledge of the substrate for the particular enzyme under study, while for a vast number of enzymes (especially for proteolytic enzymes) the identity of their targets is not known.[12] Third, the major challenge in the fabrication of enzyme biosensors arises from the intrinsic instability of the protein of interest under the conditions used to immobilize it to the transducer surface.[13] Finally, the compatibility of these biosensors with current proteomic analysis methods has been only limitedly shown,[14] and retrieval of the trapped protein fragments for downstream mass spectrometry (MS) analysis, which is highly important for understanding the biological roles of proteolytic enzymes, has not been demonstrated.

Common methods to asses enzymes activity and identify protein digestion fragments include colorimetric[15] and immunological assays,[16] as well as fluorescent[17] and radio-

Received: December 11, 2012
Accepted: December 26, 2012

   dx.doi.org/10.1021/ac303597w | *Anal. Chem.* XXXX, XXX, XXX–XXX

labeling.[18] All of these methods, particularly when used in combination with chromatography and mass spectrometry, offer high selectivity, reproducibility, and sensitivity. However, they are limited by the need for meticulous sample preparation and manipulation prior to analysis.[19,20] Therefore, there is a need for novel biosensing platforms that can integrate minute sample use and enzyme regeneration, ease of detection, and precise characterization of the product, allowing for fast and high-throughput analysis of small-volume samples with minimal losses.[21]

Here we report a versatile design of a PSi nanostructure-based biosensor, which takes advantage of DNA-directed immobilization (DDI) and allows postreaction MS analysis. DDI, which uses single-stranded DNA as a linker for specific immobilization based on Watson−Crick base pairing with complementary DNA attached to the protein, has already been used for successful immobilization of different classes of enzymes.[21−26] Given that DNA hybridization is a reversible process, the anchored enzyme can be regenerated and reused for multiple reaction cycles by applying relatively mild procedures, such as elevated temperatures or base treatments.[21]

EXPERIMENTAL SECTION

Materials. Highly doped p-type Si wafers (0.0008 Ω·cm resistivity, ⟨100⟩ oriented, B-doped) are purchased from Siltronix Corp. Aqueous HF (48%) and ethanol absolute are supplied by Merck. 3-Aminopropyl(triethoxyl)silane (APTES), glutaric dialdehyde (50 wt %), horseradish peroxidase (HRP) type VI, trypsin from bovine pancreas (treated with L-1-tosylamido-2-phenylethyl chloromethyl ketone, TPCK), 1,4-dithiothreitol (DTT), *N*,*N*-dimethylformamide (DMF), Ampliflu red, *N*α-benzoyl-L-arginine ethyl ester (BAEE), 5′-thiolated and 5′-amine modified oligonucleotides, and analytical grade buffers are purchased from Sigma-Aldrich Chemicals. Sulfo-succinimidyl-4-(*N*-maleimido-methyl)cyclohexane-1-carboxylate (sSMCC) is obtained from Pierce.

Preparation of Porous SiO_2 Nanostructures. Single-side polished on the ⟨100⟩ face oriented and heavily doped p-type Si wafers are electrochemically etched in a 3:1 (v/v) solution of aqueous HF and ethanol at a constant current density of 500 mA cm^{-2} for 11 s. *CAUTION*: HF is a highly corrosive liquid, and it should be handled with extreme care. Si wafers with an exposed area of 1.33 cm^2 are contacted on the backside with a strip of aluminum foil and mounted in a Teflon etching cell; a platinum mesh is used as the counter electrode. After etching, the surface of the wafer is rinsed with ethanol several times and dried under a dry nitrogen gas. The freshly etched PSi samples are thermally oxidized in a tube furnace (Thermolyne) at 800 °C for 1 h in ambient air, resulting in a porous SiO_2 ($PSiO_2$) layer.

Preparation of HRP and Trypsin DNA Conjugates. To prepare the HRP−DNA conjugate, 100 μL of a 100 μM solution of 5′-thiol modified oligonucleotide sscDNA in TE buffer is mixed with 60 μL of DTT (1 M) and incubated overnight at 37 °C to reduce any disulfide bonds formed upon storage of the oligonucleotide. An amount of 0.92 mg of HRP is dissolved in 200 μL of phosphate buffer (50 mM, pH 7.4) and incubated for 1 h at 37 °C with sSMCC (2 mg in 60 μL of DMF). Both the DNA and the protein reaction mixtures are purified by two consecutive gel filtration chromatography steps using NAP5 and NAP10 columns (Pharmacia). The purified DNA and protein solutions, each of which had a volume of 1.5 mL, are combined and incubated in the dark at room temperature for 3 h. The reaction mixture is concentrated to ∼300 μL by ultrafiltration (Centricon 30, Millipore), and the buffer is changed to Tris (20 mM, pH 8.3) during this step. The conjugate is purified by anion-exchange chromatography on a MonoQ HR 5/5 column (Pharmacia) using a linear gradient over 25 min (AKTA purifier, Amersham Bioscience; buffer A, 20 mM Tris, pH 8.3, and buffer B, 20 mM Tris and 1.5 M NaCl, pH 8.3). The concentration is determined spectrophotometrically. Trypsin−DNA conjugates are prepared using the same conditions.

Biofunctionalization of $PSiO_2$. The $PSiO_2$ films are first immersed in a solution of APTES dissolved in toluene (43 mM) for 1 h. The samples are then extensively rinsed with toluene, methanol, acetone, and dried under a nitrogen gas. Following this step, the silanized $PSiO_2$ are incubated with a glutaraldehyde aqueous solution (2.5 wt %) for 30 min. The samples are then rinsed with water and dried with a nitrogen gas. Immediately after, DNA cross-linking is initiated, as the functionality of glutaraldehyde tends to degrade upon exposure to air. The sequence of the capture strand oligo is 5′-amino TCCTGTGTGAAATTGTTATACGCC-3′. A 100 μM solution (2 μL) of the amino-modified probe is applied onto the $PSiO_2$ surface and incubated for 2 h in a humidity chamber, followed by a postcleaning process. Finally, 2 μL of the complementary strand modified-enzyme conjugates, 2.6 μM DNA−HRP and 4.6 μM DNA−trypsin conjugates, are incubated onto the $PSiO_2$ for 30 min. Afterward, the $PSiO_2$ samples are rinsed with 50 mM PBS, soaked in the buffer for 20 min, and vigorously rinsed again with PBS to remove any unbounded species from surface.

All processes are carried out at a room temperature (RT), below the melting temperature of the DNA. Mild basic conditions are used for dissociation of the hybridized complex, thus enabling a fast surface regeneration.

Enzymatic Activity. *HRP Activity:* Ampliflu red stock solutions are prepared by using 50 mM PBS buffer (pH 7.4). Final concentrations of 1 mM H_2O_2 and 0.1 mM Ampliflu red are used to characterize the HRP activity levels. Stock solution (200 μL) is placed on the HRP-modified $PSiO_2$ sample, and the reaction progress is monitored for 8 min at RT. The fluorescence values of the reaction product resorufin are recorded at 590 nm, by using an excitation wavelength of 530 nm.

Trypsin Activity: The activity of trypsin conjugate is studied by placing a 0.5 mM BAEE solution (200 μL) in a 50 mM Tris−HCl buffer (pH 8.0). The resulting product, *N*α-benzoyl-L-arginine, is analyzed by a plate reader with UV detection at a wavelength of 253 nm for 8 min at RT. Note: All primary data are normalized to its activity in a solution by using the equivalent volumes and concentrations.

Proteolytic Activity: The $PSiO_2$ is washed with 0.1 M HEPES buffer solution pH 8.2 for 20 min. Then, 1 mg mL^{-1} of BSA in 0.1 M HEPES buffer is introduced and continually cycled through the flow cell for 80 min. Finally, the surface is washed with HEPES buffer for the removal of the entrapped proteins and fragments. The experiments are conducted at 37 °C, which is the optimal temperature for trypsin activity.

Scanning Electron Microscopy. High-resolution scanning electron microscopy (HRSEM) of the neat $PSiO_2$ is performed using a Carl Zeiss Ultra Plus HRSEM, at an accelerating voltage of 1 keV.

Optical Measurements. Interferometric reflectance spectra of $PSiO_2$ samples are collected using an OceanOptics CCD

dx.doi.org/10.1021/ac303597w | *Anal. Chem.* XXXX, XXX, XXX−XXX

USB 4000 spectrometer fitted with a microscope objective lens coupled to a bifurcated fiber-optic cable. A tungsten light source is focused onto the center of the sample surface with a spot size of approximately 1−2 mm^2. Reflectivity data are recorded in the wavelength range of 400−1000 nm, with a spectral acquisition time of 100 ms. Both illumination of the surface and detection of the reflected light are performed along an axis coincident with the surface normal. All the optical experiments are conducted in a fixed cell in order to ensure that the sample's reflectivity is measured at the same spot during all the measurements. All optical measurements are collected in aqueous surrounding. Spectra are collected using a CCD spectrometer and analyzed by applying fast Fourier transform (FFT), as previously described.[27]

MS Analysis. The retrieved fragments (aliquots of 2 μL) are performed by using a nanoelectrospray ionization (ESI) quadrupole time-of-flight instrument (Applied Biosystems, Foster City, CA). Proteomic analysis of the separated peptides is performed by ESI-MS/MS. Detailed characterization data is described in the Supporting Information.

RESULTS AND DISCUSSION

Biofunctionalization of $PSiO_2$ with DNA−Enzyme Conjugates. PSi Fabry−Pérot thin films are synthesized from a highly doped p-type single-crystal Si wafer using anodic electrochemical etch followed by thermal oxidation to generate a stable and a more hydrophilic porous SiO_2 ($PSiO_2$) nanostructure.[28] Figure 1 (top) shows HRSEM images of a typical, highly porous substrate with interconnecting cylindrical pores of 60−80 nm in diameter. Immobilization of the enzymes onto the $PSiO_2$ nanostructure by means of DDI is carried out using a four-step process, as schematically illustrated in Figure 1 (bottom). First, the $PSiO_2$ is aminosilanized using APTES, and free amino groups are functionalized with glutaraldehyde (GluAld) to obtain an activated surface (Figure 1c). Then, the amine-modified capture complementary DNA (sscDNA) is grafted on the surface (Figure 1d) to serve as an anchor for the attachment of two different classes of enzymes. As a proof of concept, HRP, one of the most powerful peroxidases, is used first.[29,30] Once the methodology is established, the activity of trypsin, a biologically relevant protease and one of the most widely used enzymes for peptide mapping (see the Supporting Information for enzymes characteristics), is investigated.[31,32] Enzyme−DNA conjugates are synthesized by covalent coupling strategy using a bifunctional cross-linker containing maleimide and NHS ester moieties to enable attachment of thiolated DNA onto Lys residues of the protein.[13,33] In the final step, DNA−enzyme conjugates are hybridized with complementary capture oligonucleotides to enable their immobilization onto the $PSiO_2$ surface (Figure 1e). The attachment is confirmed by reflective interferometric Fourier transform spectroscopy (RIFTS), which is sensitive to small changes in the average refractive index of the film, and by measurement of the effective optical thickness (EOT) of the $PSiO_2$ thin film.[27] Figure 2 depicts significant EOT changes after each of the above-described immobilization steps, corresponding to an increase in the average refractive index. It should be noted that the EOT values observed after each modification are normalized to the EOT value of the APTES-modified $PSiO_2$ surface. In order to confirm the enzyme immobilization occurs solely through hybridization, nonmodified HRP (neat enzyme) is incubated with the amine sscDNA-modified $PSiO_2$. Indeed, insignificant EOT changes are observed in this case (data not shown). Thus, the RIFTS

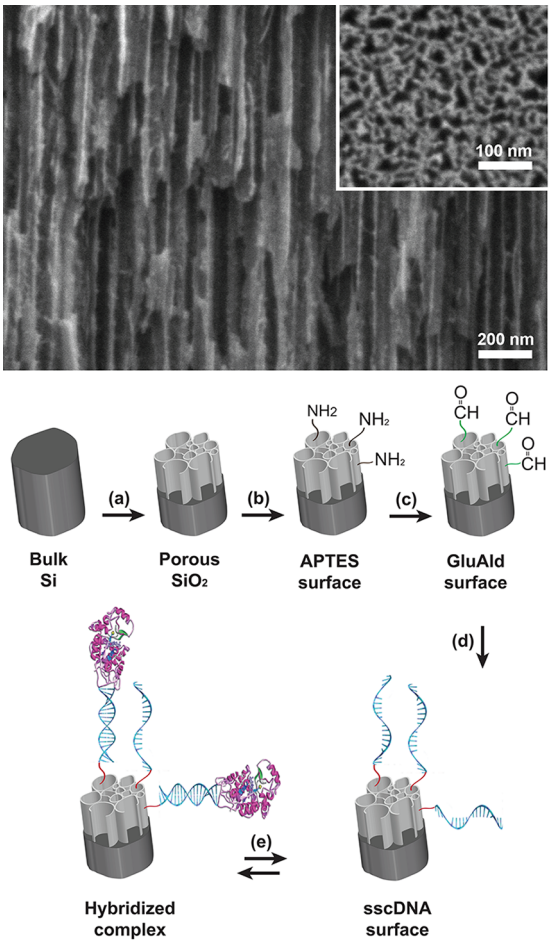

Figure 1. Top: HRSEM micrographs of a typical $PSiO_2$ film. The inset shows a top view of the porous surface. Bottom: a schematic representation of the synthetic steps required for enzyme immobilization onto PSi. (a) Si wafer is electrochemically etched at a current density of 500 mA cm^{-2} for 11 s. The resulting porous film is thermally oxidized to yield a SiO_2 surface; (b) the $PSiO_2$ surface modification with APTES; (c) the amine-terminated surface reacts with glutaraldehyde (GluAld) cross-linker; (d) grafting of amine−sscDNA onto the surface; (e) DNA−enzyme conjugate hybridization to the anchored sscDNA surface. Note: These schematics are for illustration purposes only as all modifications occur also inside the porous layer.

results confirm that the enzyme immobilization onto the $PSiO_2$ surface occurs through Watson−Crick base pairing.

Enzymatic Activity Assays. To assess the enzymatic activity of the enzymes anchored onto the $PSiO_2$, the substrate oxidation ability of HRP and proteolytic activity of trypsin are first examined using colorimetric assays. Modified $PSiO_2$ surfaces are exposed to the corresponding substrates, allowed to react, and collected for spectrophotometric analysis. Figure 3b shows the results of the enzymatic assay for the immobilized conjugates. Both enzymes exhibit high relative activity when anchored onto the $PSiO_2$. Values of 78% and 85% are obtained for trypsin and HRP, respectively, compared to the enzyme activity in solution. It should be noted that relative activity of the enzyme conjugates is compared assuming that all enzyme molecules are immobilized onto the porous nanostructure. Thus, the values in Figure 3b underestimate the enzymatic activity of the immobilized conjugates. Remarkably, the concentrations of the enzymes we use are at least 1 order of

dx.doi.org/10.1021/ac303597w | Anal. Chem. XXXX, XXX, XXX−XXX

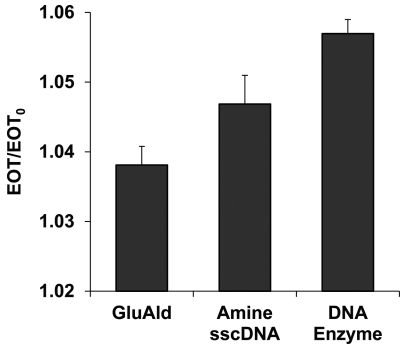

Figure 2. EOT values at different steps throughout the enzyme–conjugate (HRP) immobilization onto $PSiO_2$. The immobilization process includes four steps: (i) APTES modification (termed as EOT_0); EOT data are normalized to this initial value; (ii) aldehyde-modified porous surface (GluAld); (iii) amine-modified sscDNA is reacted with the surface, (iv) followed by hybridization of the complementary ssDNA–HRP conjugate. Note: the EOT values of various modifications are normalized to the EOT value of the aminosilane-modified $PSiO_2$ surface (APTES).

magnitude lower compared to the previous studies reported in the literature. Orosco et al.[6] have used initial pepsin concentration of 1 mg mL^{-1} in comparison to 0.1 mg mL^{-1} of HRP and trypsin conjugates used in this study.

An important advantage of the DDI anchoring is the ability of surface regeneration by use of mild dehybridization conditions. As shown in Figure 3, the enzymes can be removed from the $PSiO_2$ surface as indicated by the negligible enzymatic activity (less than 1%) after mild basic wash (Figure 3c). In addition, a consecutive cycle of hybridization/dehybridization is carried out to demonstrate the reversibility of the enzyme attachment and the ability for its retrieval and reuse. These experiments clearly show the high reversibility and reproducibility of this immobilization strategy as >60% and <1% of relative activity, before and after dehybridization, respectively, are measured for both HRP and trypsin (Figure 3, parts b and c).

Optical Detection of Enzymatic Activity. Once it is shown that both trypsin–DNA and HRP–DNA conjugates remain catalytically active after the attachment onto $PSiO_2$ nanostructures, we investigate the potential of this platform to act as an optical biosensor for monitoring protease activity and allowing downstream MS analysis. Thus, trypsin-modified $PSiO_2$ is fixed in a flow cell setup and exposed to various substrate/buffer combinations. The reactions are monitored in real time by acquisition of the reflectivity spectra from the porous thin film, and the recorded normalized EOT values provide a direct measure of the amount of digestion products—peptides infiltrating the pores. Figure 4 shows the normalized EOT changes of trypsin-modified $PSiO_2$ following the introduction of bovine serum albumin (BSA). A rapid increase of approximately 0.12% in the EOT value is observed (Figure 4b), which is attributed to the infiltration and accumulation of BSA in the nanostructure (characterized by 60–80 nm diameter pores). Subsequent gradual increase is observed until the EOT value attains a plateau (Figure 4b). This increase is mainly ascribed to the proteolytic reaction occurring within the porous scaffold and also to additional infiltration of BSA.[6] When HEPES buffer is introduced into the flow cell, a rapid decrease in EOT occurs (Figure 4c), which is attributed to the

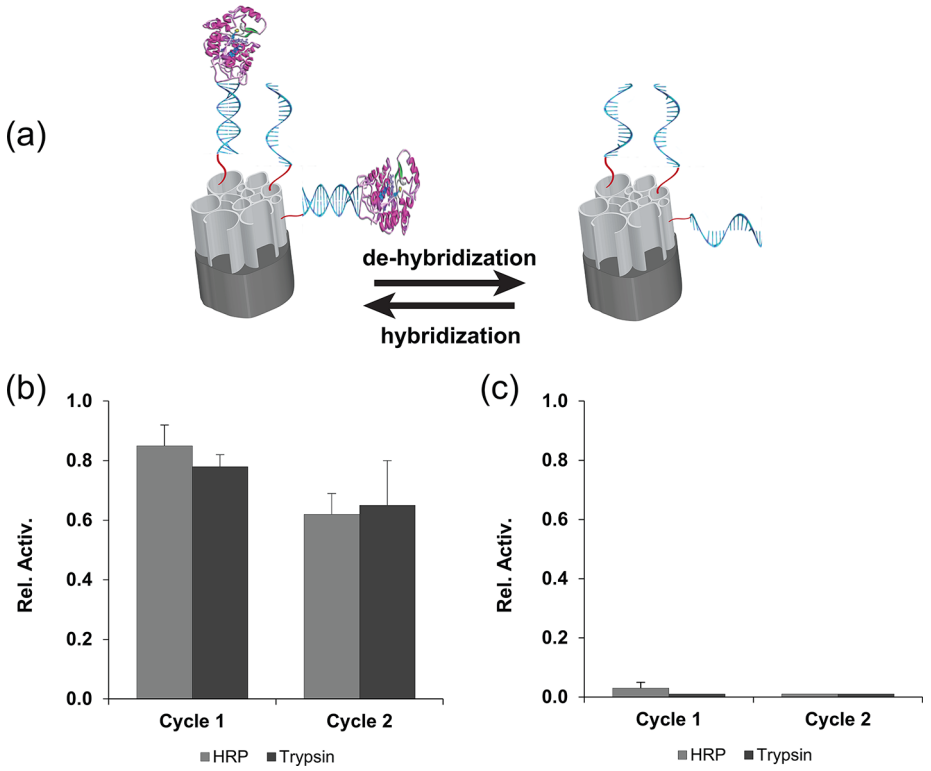

Figure 3. (a) Schematic illustration of reversible enzyme immobilization onto a $PSiO_2$ surface using the DDI approach. (b) Relative activity of trypsin and HRP, immobilized via DDI onto $PSiO_2$. (c) Mild dehybridization allows removal of the DNA–enzyme conjugates from the surface. Two consecutive cycles of DNA–enzyme hybridization/dehybridization are preformed to demonstrate the high reversibility and reproducibility of this immobilization strategy.

dx.doi.org/10.1021/ac303597w | *Anal. Chem.* XXXX, XXX, XXX–XXX

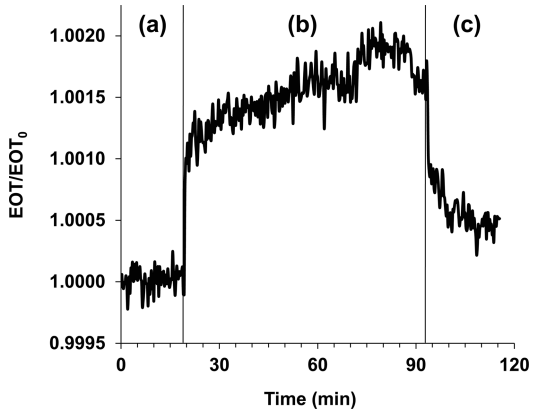

Figure 4. Optical response of trypsin-modified $PSiO_2$ nanostructures upon BSA introduction. The trypsin-modified $PSiO_2$ nanostructure is pretreated with 0.1 M PBS, pH 7.4 to minimize nonspecific adsorption of proteins. (a) Wash with 0.1 M HEPES buffer pH 8.2, no change in the EOT is observed; (b) addition of 1 mg mL^{-1} of BSA in 0.1 M HEPES buffer is introduced; (c) HEPES buffer wash step. The $PSiO_2$ biosensor is fixed in a custom-made flow cell, and the reflectivity spectra are recorded every 15 s.

removal of BSA and its digestion fragments from the nanostructure. Control experiments with neat $PSiO_2$ (no enzyme) and HRP-modified $PSiO_2$, subjected to similar BSA concentrations, show only the initial rapid increase in EOT due to BSA adsorption (data not shown). The second increase in EOT, which we attribute to the accumulation of the digestion products in the pores, is not observed, indicating that the biosensor platform is indeed specific for monitoring the proteolytic activity.

MS Analysis. As already mentioned, a key requirement for the protease biosensor is the ability to retrieve generated peptides for sequence identification by proteomic analysis. Such examination does not only allow the insight into the substrate specificity but it also enables identification of the proteolytic cleavage site. To demonstrate that this is indeed possible with our biosensing platform, BSA and myoglobin proteins are digested using the trypsin–$PSiO_2$ under both native and denatured conditions. The resulting peptides are retrieved from the nanostructure by buffer wash, and tandem proteomic analysis is carried out (Figure 5 and Supporting Information Figures S1 and S2). The results show that unique identification of both proteins (BSA and myoglobin) is possible by peptide sequence analysis. As expected from the trypsin activity profile, all generated peptides contained N-terminal lysines or arginines (see Figure 5e and Supporting Information Figure S1). Moreover, the results clearly show that more efficient degradation and hence higher sequence coverage is obtained under denaturing conditions, due to better accessibility of the protein to the proteolytic sites (Supporting Information Figure S2). Thus, for the first time, the compatibility of $PSiO_2$-based enzyme biosensors with tandem MS techniques is established.

CONCLUSIONS

A biosensing platform is designed for investigation of the enzymatic activity of proteases. The specific and reversible nature of the enzyme immobilization strategy employed in this work enables the use of minute sample quantities, and the simplicity of the readout procedure provides real-time tracking of the reaction. Thus, this methodology offers an unbiased approach for substrate recognition and cleavage site identification. Given that, to date, the substrate degradome of hundreds of proteases remains unknown, we believe that such a platform will be of practical importance for substrate profiling.[34] It should be emphasized that the presented generic platform can be tailored and applied for the study of many other protein classes.

ASSOCIATED CONTENT

Supporting Information

Additional information as noted in text. This material is available free of charge via the Internet at http://pubs.acs.org.

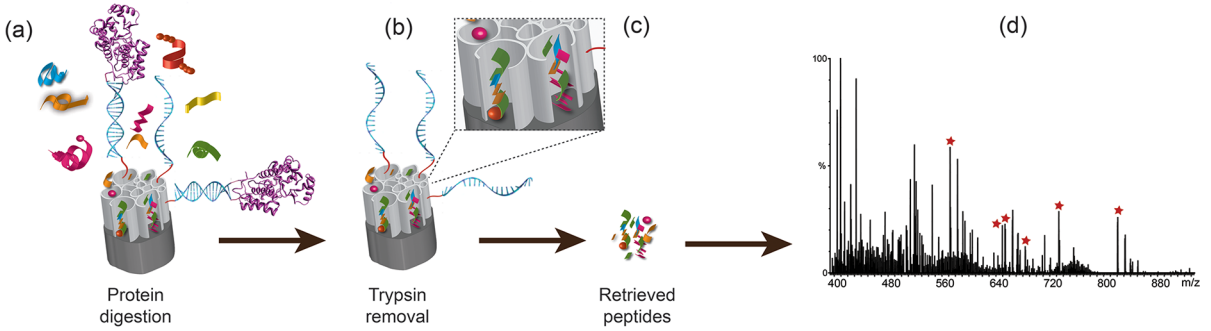

(e)

```
  1 MKWVTFISLL LLFSSAYSRG VFRRDTHKSE IAHRFKDLGE EHFKGLVLIA
 51 FSQYLQQCPF DEHVKLVNEL TEFAKTCVAD ESHAGCEKSL HTLFGDELCK
101 VASLRETYGD MADCCEKQEP ERNECFLSHK DDSPDLPKLK PDPNTLCDEF
151 KADEKKFWGK YLYEIARRHP YFYAPELLYY ANKYNGVFQE CCQAEDKGAC
201 LLPKIETMRE KVLASSARQR LRCASIQKFG ERALKAWSVA RLSQKFPKAE
251 FVEVTKLVTD LTKVHKECCH GDLLECADDR ADLAKYICDN QDTISSKLKE
301 CCDKPLLEKS HCIAEVEKDA IPENLPPLTA DFAEDKDVCK NYQEAKDAFL
351 GSFLYEYSRR HPEYAVSVLL RLAKEYEATL EECCAKDDPH ACYSTVFDKL
401 KHLVDEPQNL IKQNCDQFEK LGEYGFQNAL IVRYTRKVPQ VSTPTLVEVS
451 RSLGKVGTRC CTKPESERMP CTEDYLSLIL NRLCVLHEKT PVSEKVTKCC
501 TESLVNRRPC FSALTPDETY VPKAFDEKLF TFHADICTLP DTEKQIKKQT
551 ALVELLKHKP KATEEQLKTV MENFVAFVDK CCAADDKEAC FAVEGPKLVV
601 STQTALA
```

Figure 5. Schematic illustration of the protease biosensor: (a) digestion of BSA by immobilized trypsin; (b) removal of trypsin from the biosensor (inset shows a magnification of the porous area); (c) retrieval of the trapped peptide fragments; (d) MS spectrum of the retrieved BSA fragments; (e) amino acid sequence of BSA. Sequences in bold reflect the identified peptides in the LC–MS/MS analysis.

dx.doi.org/10.1021/ac303597w | Anal. Chem. XXXX, XXX, XXX–XXX

AUTHOR INFORMATION

Corresponding Author

*E-mail: ljiljana.fruk@kit.edu (L.F.); esegal@tx.technion.ac.il (E.S.). Phone: +49-721-60845800 (L.F.); +972-4-8295071 (E.S.). Fax: +49-721-60848495 (L.F.); +972-4-8293399 (E.S.).

Author Contributions

G.S. carried out PSi synthesis, enzyme immobilization, enzyme activity assays, biosensing experiments, and data analysis. He also wrote the manuscript. N.M.-I. has contributed to the conception of the experiments and has been involved in the synthesis and characterization of PSi. S.E. has synthesized the DNA−enzyme conjugates. O.M. and M.S. have participated in the design of the study. L.F. conceived the study and coordinated the synthesis and characterization of DNA−enzyme conjugates. E.S. conceived and coordinated the study, participated in the design of the study and data analysis, and drafted the manuscript. All authors read and approved the final manuscript.

Notes

The authors declare no competing financial interests.

ACKNOWLEDGMENTS

This work is partially supported by the KIT−Weizmann Institute−Technion Multidisciplinary Research in Nanoscience Program. M.S. is the incumbent of the Elaine Blond Career Development Chair and the support of the European Research Council (ERC), Grant Agreement No. 239679. L.F. is grateful to the KIT Excellence initiative, CFN project A5.7. E.S. acknowledges the support of the Marie Curie Reintegration Grant (NANOPACK) administered by the European Community.

REFERENCES

(1) Jane, A.; Dronov, R.; Hodges, A.; Voelcker, N. H. *Trends Biotechnol.* **2009**, *27* (4), 230−239.

(2) Pacholski, C.; Sartor, M.; Sailor, M. J.; Cunin, F.; Miskelly, G. M. *J. Am. Chem. Soc.* **2005**, *127* (33), 11636−11645.

(3) DeLouise, L. A.; Kou, P. M.; Miller, B. L. *Anal. Chem.* **2005**, *77* (10), 3222−3230.

(4) Sailor, M. J. *ACS Nano* **2007**, *1* (4), 248−252.

(5) Orosco, M. M.; Pacholski, C.; Miskelly, G. M.; Sailor, M. J. *Adv. Mater.* **2006**, *18* (11), 1393−1396.

(6) Orosco, M. M.; Pacholski, C.; Sailor, M. J. *Nat. Nanotechnol.* **2009**, *4* (4), 255−258.

(7) Kilian, K. A.; Boecking, T.; Gaus, K.; Gal, M.; Gooding, J. J. *ACS Nano* **2007**, *1* (4), 355−361.

(8) Bocking, T.; Kilian, K. A.; Gaus, K.; Gooding, J. J. *Adv. Funct. Mater.* **2008**, *18* (23), 3827−3833.

(9) Kilian, K. A.; Boecking, T.; Gooding, J. J. *Chem. Commun.* **2009**, *6*, 630−640.

(10) Tanaka, T.; Yada, R. Y. *Biochem. J.* **1996**, *315*, 443−446.

(11) Bao, J. J.; Fujima, J. M.; Danielson, N. D. *J. Chromatogr., Biomed. Appl.* **1997**, *699* (1), 481−497.

(12) Turk, B. *Nat. Rev. Drug Discovery* **2006**, *5* (9), 785−799.

(13) Fruk, L.; Muller, J.; Weber, G.; Narvaez, A.; Dominguez, E.; Niemeyer, C. M. *Chem.—Eur. J.* **2007**, *13* (18), 5223−5231.

(14) Tan, J.; Zhao, W.-J.; Yu, J.-K.; Ma, S.; Sailor, M. J.; Wu, J.-M. *Adv. Healthcare Mater.* **2012**, *1* (6), 742−750.

(15) Lin, H. J.; Lien, Y. C.; Hsu, C. H. *Anal. Biochem.* **2010**, *407* (2), 226−232.

(16) Fournout, S.; Roquet, F.; Salhi, S. L.; Seyer, R.; Valverde, V.; Masson, J. M.; Jouin, P.; Pau, B.; Nicolas, M.; Hanin, V. *Anal. Chem.* **1997**, *69* (9), 1746−1752.

(17) Basak, A.; Chretien, M.; Seidah, N. G. *FEBS Lett.* **2002**, *514* (2−3), 333−339.

(18) Rucklidge, G. J.; Milne, G. *Anal. Biochem.* **1990**, *185* (2), 265−269.

(19) Marnett, A. B.; Craik, C. S. *Trends Biotechnol.* **2005**, *23* (2), 59−64.

(20) Overall, C. M.; Blobel, C. P. *Nat. Rev. Mol. Cell Biol.* **2007**, *8* (3), 245−257.

(21) Shtenberg, G.; Massad-Ivanir, N.; Engin, S.; Sharon, M.; Fruk, L.; Segal, E. *Nanoscale Res. Lett.* **2012**, *7*, 443.

(22) Fruk, L.; Niemeyer, C. M. *Angew. Chem., Int. Ed.* **2005**, *44* (17), 2603−2606.

(23) Wacker, R.; Niemeyer, C. M. *ChemBioChem* **2004**, *5* (4), 453−459.

(24) Kuo, C. H.; Fruk, L.; Niemeyer, C. M. *Chem.—Asian J.* **2009**, *4* (7), 1064−1069.

(25) Niemeyer, C. M.; Ceyhan, B. *Angew. Chem., Int. Ed.* **2001**, *40* (19), 3685−3688.

(26) Niemeyer, C. M. *Angew. Chem., Int. Ed.* **2010**, *49* (7), 1200−1216.

(27) Massad-Ivanir, N.; Shtenberg, G.; Tzur, A.; Krepker, M. A.; Segal, E. *Anal. Chem.* **2011**, *83* (9), 3282−3289.

(28) Segal, E.; Perelman, L. A.; Cunin, F.; Di Renzo, F.; Devoisselle, J. M.; Li, Y. Y.; Sailor, M. J. *Adv. Funct. Mater.* **2007**, *17* (7), 1153−1162.

(29) Zhang, J. D.; Chi, Q. J.; Dong, S. J.; Wang, E. K. *Bioelectrochem. Bioenerg.* **1996**, *39* (2), 267−274.

(30) Loew, N.; Bogdanoff, P.; Herrmann, I.; Wollenberger, U.; Scheller, F. W.; Katterle, M. *Electroanalysis* **2006**, *18* (23), 2324−2330.

(31) Ren, D.; Pipes, G. D.; Liu, D. J.; Shih, L. Y.; Nichols, A. C.; Treuheit, M. J.; Brems, D. N.; Bondarenko, P. V. *Anal. Biochem.* **2009**, *392* (1), 12−21.

(32) Min, Q. H.; Wu, R. A.; Zhao, L. A.; Qin, H. Q.; Ye, M. L.; Zhu, J. J.; Zou, H. F. *Chem. Commun.* **2010**, *46* (33), 6144−6146.

(33) Niemeyer, C. M.; Sano, T.; Smith, C. L.; Cantor, C. R. *Nucleic Acids Res.* **1994**, *22* (25), 5530−5539.

(34) Schilling, O.; Overall, C. M. *Curr. Opin. Chem. Biol.* **2007**, *11* (1), 36−45.